A computational study of tunneling-percolation electrical transport in graphene-based nanocomposites

Jeremy Hicks,[a] Ashkan Behnam, and Ant Ural[b]
Department of Electrical and Computer Engineering, University of Florida, Gainesville, Florida 32611 USA

(Received 6 July 2009; accepted 26 October 2009; published online 24 November 2009)

Using a tunneling-percolation model and Monte Carlo simulations, we study the resistivity of graphene-based nanocomposites as a function of both graphene sheet and device parameters. We observe an inverse power law dependence of resistivity on device dimensions and volume fraction near the percolation threshold, and find that high aspect ratio graphene sheets result in a much lower resistivity, particularly at low sheet densities. Furthermore, we find that graphene sheet area affects nanocomposite resistivity more strongly than sheet density does. These results impart important fundamental insights for future experimental investigations and applications of graphene-based conductive nanocomposites. © *2009 American Institute of Physics*. [doi:10.1063/1.3267079]

Thin films formed by large networks of individual graphene sheets and composites created by the incorporation of those sheets into bulk insulating materials such as polystyrene[1,2] and silica[3] have recently attracted significant research attention for having demonstrated, simultaneously, high conductivity and transparency[1–4] as well as excellent flexibility.[5] Crucially, they have been manufactured using inexpensive chemical processes,[1–4] with the constituent graphene being produced inexpensively using methods ranging from the chemical reduction of oxygenated graphene (graphene oxide)[1–4] to chemical vapor deposition,[5,6] making them appealing in low-cost applications. The incorporation of graphene sheets into polymer or ceramic matrices has the potential for significant improvements in their properties. Potential uses may include thin, flexible electrodes, transparent conductors, and lightweight, rugged structural composites.[1–6]

Electrical transport in graphene-based nanocomposites can be well-described by tunneling-percolation through conducting, pseudo-two-dimensional (2D) graphene sheet elements, owing to graphene's exceptional basal plane charge mobilities that surpass 25 000 cm^2/Vs (Ref. 7) and weak out-of-plane interactions,[8] limiting the conduction between sheets separated by the insulating matrix to be orders of magnitude worse. Furthermore, there are significant experimental data showing the composite resistivity exhibits behavior characteristic of percolation networks when plotted versus graphene percent composition.[1,3] While there is abundant literature on the general topic of percolation thresholds in networks composed of 2D elements,[9,10] the work on their electrical characteristics is less expansive. Furthermore, although several recent works have demonstrated the fabrication of graphene-based nanocomposites experimentally,[1–6] modeling/simulation of their electrical properties has not been performed previously.

In this letter, we develop a tunneling-percolation model using Monte Carlo simulations to investigate electrical transport in graphene-based nanocomposites. After comparing the model to experiment, we present the effect of sheet aspect ratio on composite resistivity, finding that high aspect ratio sheets result in a much lower resistivity, particularly when the number of sheets is small. Next, we show an inverse power law dependence of resistivity on device width and thickness near the percolation threshold and extract the associated critical exponents. Finally, we explore the relative contributions of graphene sheet density and area, finding that sheet area affects nanocomposite resistivity more strongly than sheet density, suggesting that nanocomposites composed of larger sheets are better for device applications.

To study the electrical characteristics of graphene-based nanocomposites, we employ Monte Carlo simulations [exemplified in Fig. 1(a)] and model the networks as comprised of charge percolating, randomly dispersed rectangles parallel to the substrate at an essentially continuous set of heights above it, since experiments suggest that graphene sheets in composites mostly align themselves to the substrate.[2,3] The percolation model used for each sheet is the "permeable shell, hard core" model, which in this case denotes a network of impenetrable rectangular prism-shaped objects (the hard core) that are surrounded by a uniform, penetrable boundary (the permeable shell). Physically, the core corresponds to the physical extent of each graphene element while the permeable shell represents the effective tunneling distance extending out from the element's interior. In our simulations, we assign a hard core thickness of 1 nm to account for the fact that graphene sheets encased in composites exhibit, in contrast to individual graphene sheets lying on a flat substrate, a highly "crumpled" nature whose bending causes the graphene to assume an effective thickness profile on the order of 1 nm rather than angstroms.[1,3] The permeable shell extends another 1 nm beyond the core for a maximum tun-

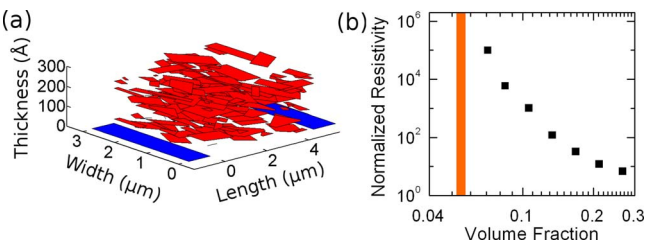

FIG. 1. (Color online) (a) A representative network of simulated graphene sheets in a nanocomposite. The darker shaded regions at either end indicate source/drain electrodes. (b) Resistivity as a function of graphene sheet volume fraction, observing the characteristic inverse power law behavior of percolation systems. The device dimensions are 3 μm in width, 5 μm in length, and 30 nm in thickness with sheet areas of 0.5 μm^2. The vertical line represents the location of the critical volume fraction v_c.

[a]Present Address: Georgia Institute of Technology, Atlanta, GA.
[b]Electronic mail: antural@ufl.edu.

neling distance of 3 nm between sheet centers. Additionally, we assume that the resistivity in the networks is dominated by sheet-sheet junction resistances by the above statement of significant anisotropy in the conductivity of graphene sheets and the high tunneling junction resistances through the insulating matrix.

For these simulations, we employ a formula for tunneling current density between two electrodes under an intermediate bias derived by Simmons[11,12] to find the sheet-sheet junction resistances R_J as

$$R_J = \frac{V}{A_J J_0\{\varphi_1 \exp(-K\sqrt{\varphi_1}) - (\varphi_1 + eV)\exp(-K\sqrt{\varphi_1 + eV})\}}, \quad (1)$$

where V is the voltage bias, A_J is the contact area, φ_1 is the mean tunnel barrier height, e is electronic charge, and J_0 is an arbitrary constant. Furthermore, $K=4\pi\Delta s\sqrt{2m/h}$, where h is Planck's constant, m is the electron mass, and Δs is the difference between the limits of the barrier at the Fermi level. Finally, φ_1 is shaped by the electrode material work function as well as the dielectric constant of the insulator comprising the barrier, and so we assume a graphene sheet work function of 4.5 eV (Ref. 4) and that the insulating matrix material is polystyrene (dielectric constant $\varepsilon_r \approx 2.5$).

After the graphene sheet network is generated, the junctions between sheets are then found and the junction overlap areas are calculated. This information is compiled into an adjacency matrix whose elements A_{ji} contain information about R_{ji}, the junction resistance between graphene sheets i and j. Kirchhoff's current law is then imposed to calculate the resistivity of the network by solving a set of nodal equations for the junction potentials.[13,14] Finding the potential V_j for each sheet means solving either $\Sigma_i(V_i-V_j)/R_{ji}=0$ if j is not adjacent to either the source or drain, or $\Sigma_i(V_i-V_j)/R_{ji}=(V_j-V_{s/d})/R_{jsd}$, where $V_{s/d}$ are the prespecified source/drain potentials, respectively, and R_{jsd} is the resistance between sheet j and the source/drain. This calculation must be done self-consistently because the current density at a junction is dependent upon the potential across it.

In order to compare our model to experiment, we present in Fig. 1(b) the resistivity scaling with graphene sheet volume fraction v, defined as the ratio of the volume occupied by the graphene to the entire composite volume. The graphene volume is calculated by multiplying the total combined area of every sheet in the composite by an effective thickness of 3.35 Å—the interlayer distance in graphite. Each data point is the median of 100 simulations, with 1000 used near the percolation threshold to offset higher sample-to-sample variations in resistivity. Nanocomposite resistivity ρ near the percolation threshold exhibits the characteristic power law behavior of percolating systems, $\rho \propto (v-v_c)^{-\tau}$, where v_c is the critical volume fraction, defined here as the volume fraction at which the chance that one simulation of the composite will have at least one connection between source and drain is 50%. We find that $v_c=5.7\pm0.1\%$, resulting in an extracted $\tau=3.6\pm0.3$. This τ value is somewhat larger than, but similar to, the experimental 2.74 ± 0.2 reported by Stankovich, *et al.*[1]

Figure 2 shows nanocomposite resistivity as a function of graphene sheet aspect ratio AR ranging from one (squares) to 20 (long rectangles), fixing sheet area at 0.5 μm^2, with each data series representing a different volume fraction v.

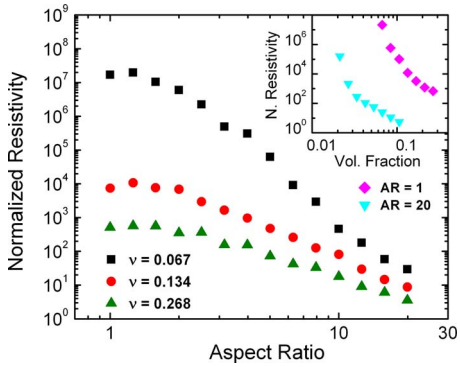

FIG. 2. (Color online) Log-log plot of resistivity as a function of graphene sheet aspect ratio (AR) for three different volume fractions. Inset: Resistivity vs. volume fraction for sheets with $AR=1$ and 20, keeping sheet area constant at 0.5 μm^2.

We observe, consistent with other studies, that high aspect ratio sheets more efficiently aid charge percolation at the same v.[10] The effect of aspect ratio on resistivity is more pronounced at lower volume fractions (i.e., closer to the percolation threshold). This can be seen better in the inset of Fig. 2, which plots resistivity as a function of volume fraction for $AR=1$ and 20. At lower v, the resistivity difference between the two data series is vast, but as the volume fraction increases, both systems are brought further away from the percolation threshold and their resistivities begin to saturate.

Because strong resistivity dependence on device dimensions has been observed experimentally for nanotube films,[15] we investigate if a similar effect exists in graphene-based nanocomposites. In Fig. 3, we plot resistivity as a function of device width W for $AR=1$ and 20 and find that the resistivity scales strongly with width for both aspect ratios as $\rho \propto (W-W_c)^{-\gamma}$, where W_c is the critical width and γ is the width critical exponent. For $AR=1$, we find $W_c=0.3\pm0.05$ μm with $\gamma=2.1\pm0.3$, and for $AR=20$, $W_c=0.15\pm0.05$ μm with $\gamma=4.1\pm0.5$. As shown in the inset, resistivity as a function of thickness t follows a similar power law $\rho \propto (t-t_c)^{-\beta}$ with $t_c=36\pm2$ and 32 ± 2 Å and $\beta=1.8\pm0.1$ and 0.8 ± 0.1 for $AR=1$ and 20, respectively. As both a function of increasing W and t, the resistivity of the nanocomposite is seen to decrease. The decrease can be explained by the fact that the transport in percolation networks occurs through many parallel conducting paths, and increas-

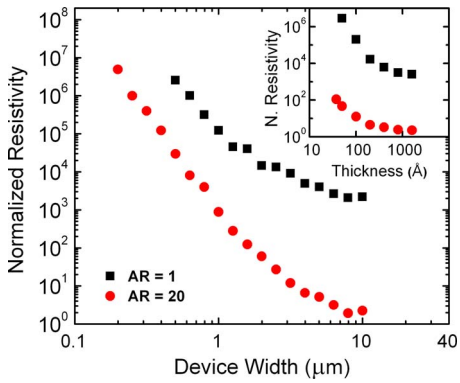

FIG. 3. (Color online) Log-log plot of resistivity as a function of device width for two different graphene sheet aspect ratios. The inset shows log-log plot of resistivity as a function of device thickness for two different aspect ratios, following a similar trend to the effect of device width.

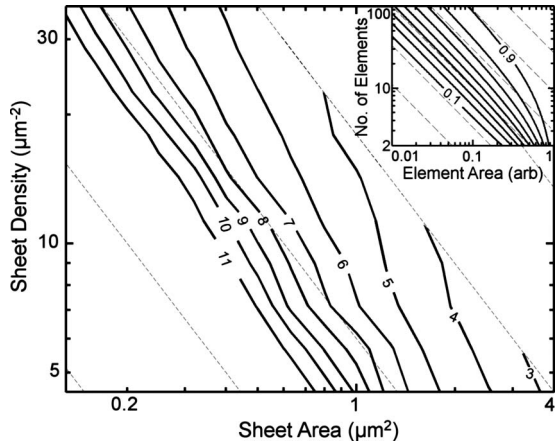

FIG. 4. Resistivity contours for a matrix of sheet areas (x-axis) and sheet densities (y-axis) for a 5 μm by 5 μm by 30 nm device. Inset: A contour plot of element-element connection probability P as a function of number of elements (N) and element area. The numbers on the contours indicate the value of P.

ing either W or t increases the number of these paths from source to drain.[13,15] Furthermore, the large difference in γ between the two different aspect ratio cases may be explained by the fact that nanocomposites composed of square sheets ($AR=1$) are more insensitive to changes in device width because their connectivity is fairly independent of sheet orientation.

Finally, we consider the relative effects of graphene sheet area and density, defined here as the number of sheets contained on a 1 μm^2 area of the device (i.e., integrated over the thickness), on nanocomposite resistivity. In Fig. 1, the volume fraction increase was achieved by increasing the graphene sheet density. Another way to change the volume fraction is to change the sheet area. Figure 4 shows a contour plot of nanocomposite resistivity as a function of sheet area (x-axis) and sheet density (y-axis). For reference, the dashed lines indicate a constant volume fraction, and the numbers on the contours indicate the decimal power of the normalized resistivities along them (i.e., 5 means $\rho=10^5$). The volume fraction at which some of the contours abruptly end is the maximum volume fraction that can be simulated taking into account the crumpled nature of the graphene sheets.

What is clear from Fig. 4 is that the resistivity contours have larger slopes than the constant volume fraction lines meaning that, for a fractional decrease in sheet area, the sheet density must be increased by some larger fraction in order to achieve the same resistivity. This result can be explained by the fact that increasing sheet density only increases the number of paths between source and drain whereas increasing sheet area does this as well as decreases the number of junctions per path. A closer inspection of Fig. 4 shows that the contours corresponding to the highest resistivities follow more closely the constant volume fraction lines, suggesting that the relative effect of area and density is not a constant. This could be understood better by inspecting the percolation probability at an element to element level. As a simple model, consider a 2D system of total device area A with N entirely permeable elements (circular in shape with radii r, for simplicity) where two elements are considered connected if the distance between their centers is less than $2r$. Neglecting system boundary effects, the probability P that an element is connected to at least one other is $P=1-(1-4\pi r^2/A)^{N-1}$, which is plotted as a contour plot on N versus element area in the inset of Fig. 4, where the dashed lines represent constant fractions of the total area A occupied by elements (which is similar to volume fraction). As in the main plot of Fig. 4, the higher numbered contours (analogous to lower resistivity) show the greatest sensitivity to element area while the lower numbered ones (analogous to higher resistivity) are visibly straight. All of the contours appear to straighten further toward large N, which is also seen in the main plot of Fig. 4. In the limit N is large and $4\pi r^2/A$ is small, $P \cong 4N\pi r^2/A$. This expression shows that a constant product of element area (πr^2) and number (N) should give the same value of P in the large number, small element area limit, as observed in Fig. 4. As a result, this simple conceptual picture of element-element connection probability can explain the trade-off between sheet area and sheet density observed in the simulations.

In summary, we have developed and compared with experiment a computational model to study the dependence of the resistivity of graphene-based nanocomposites on physical device parameters, presenting several important results. We find that the incorporation of graphene sheets with a high aspect ratio improve the nanocomposite's electrical properties significantly, which is immediately relevant to the production of transparent/conductive materials, where shaping the sheet geometry to create the desired resistivity at the least volume fraction and composite thickness possible is important. We also find that, unlike a bulk conductor, very small transverse device dimensions significantly increase the resistivity. Finally, we also observe that graphene sheet area affects nanocomposite resistivity more strongly than sheet density, suggesting that nanocomposites composed of larger sheets are better for device applications. These results provide a framework to interpret future experiments and open up the possibility to design better nanocomposites for potential applications.

This work was funded in part by the Semiconductor Research Corporation.

[1] S. Stankovich, D. A. Dikin, G. H. B. Dommett, K. M. Kohlhaas, E. J. Zimney, E. A. Stach, R. D. Piner, S. T. Nguyen, and R. S. Ruoff, Nature (London) **442**, 282 (2006).
[2] G. Eda and M. Chhowalla, Nano Lett. **9**, 814 (2009).
[3] S. Watcharotone, D. A. Dikin, S. Stankovich, R. D. Piner, I. Jung, G. H. B. Dommett, G. Evmenenko, S. Wu, S. Chen, C. Liu, S. T. Nguyen, and R. S. Ruoff, Nano Lett. **7**, 1888 (2007).
[4] X. Wang, L. Zhi, and K. Müllen, Nano Lett. **8**, 323 (2008).
[5] K. Kim, Y. Zhao, H. Jang, S. Lee, J. Kim, K. Kim, J. Ahn, P. Kim, J. Choi, and B. Hong, Nature (London) **457**, 706 (2009).
[6] X. Li, W. Cai, J. An, S. Kim, D. J. Nah, D. Yang, R. Piner, A. Velamakanni, I. Jung, E. Tutuc, S. K. Banerjee, L. Colombo, and R. S. Ruoff, Science **324**, 1312 (2009).
[7] C. Berger, Z. Song, X. Li, X. Wu, N. Brown, C. Naud, D. Mayou, T. Li, J. Hass, A. N. Marchenkov, E. H. Conrad, P. N. First, and W. A. de Heer, Science **312**, 1191 (2006).
[8] J.-C. Charlier, X. Gonze, and J.-P. Michenaud, Europhys. Lett. **28**, 403 (1994).
[9] D. Stauffer and A. Aharony, *Introduction to Percolation Theory* (Taylor and Francis, London, 1992).
[10] M. B. Isichenko, Rev. Mod. Phys. **64**, 961 (1992).
[11] J. G. Simmons, J. Appl. Phys. **34**, 1793 (1963).
[12] C. Li, E. T. Thostenson, and T.-W. Chou, Appl. Phys. Lett. **91**, 223114 (2007).
[13] A. Behnam and A. Ural, Phys. Rev. B **75**, 125432 (2007).
[14] J. Hicks, A. Behnam, and A. Ural, Phys. Rev. E **79**, 012102 (2009).
[15] A. Behnam, L. Noriega, Y. Choi, Z. Wu, A. G. Rinzler, and A. Ural, Appl. Phys. Lett. **89**, 093107 (2006).